Neutron Energy Distribution Function Reconstructed From Time-of-Flight Signals in Deuterium Gas-Puff Z-Pinch

Daniel Klir, Jozef Kravarik, Pavel Kubes, *Member, IEEE*, Karel Rezac, Sergey S. Ananev, Yuriy L. Bakshaev, Peter I. Blinov, Andrey S. Chernenko, Evgeny D. Kazakov, Valery D. Korolev, Gennadiy I. Ustroev, Libor Juha, Josef Krasa, and Andriy Velyhan

***Abstract*—The implosion of a solid deuterium gas-puff Z-pinch was studied on the S-300 pulsed power generator [A. S. Chernenko, *et al.*, Proceedings of 11th Int. Conf. on High Power Particle Beams, 154 (1996)]. The peak neutron yield above 10^{10} was achieved on the current level of 2 MA. The fusion neutrons were generated at about 150 ns after the current onset, i.e., during the stagnation and at the beginning of the expansion of a plasma column. The neutron emission lasted on average 25 ns. The neutron energy distribution function was reconstructed from 12 neutron time-of-flight signals by the Monte Carlo simulation. The side-on neutron energy spectra peaked at 2.42 $\pm$ 0.04 MeV with about 450-keV FWHM. In the downstream direction (i.e., the direction of the current flow from the anode toward the cathode), the peak neutron energy and the width of a neutron spectrum were 2.6 $\pm$ 0.1 MeV and 400 keV, respectively. The average kinetic energy of fast deuterons, which produced fusion neutrons, was about 100 keV. The generalized beam-target model probably fits best to the obtained experimental data.**

***Index Terms*—Deuterium, fusion reaction, gas puff, Monte Carlo reconstruction, neutron energy spectra, neutrons, Z-pinch.**

I. Introduction

AT PRESENT, Z-pinches are intensively researched as powerful and efficient laboratory sources of soft X-rays [1], [2]. Whereas a large number of papers is devoted to studies of EUV and soft X-ray radiation, experimental data about fast ions are rather rare. One of those very few examples is the recent measurement of an ion temperature in wire-arrays at the Z-machine [3]. The Doppler-width of iron spectral lines indicated that the ion temperature exceeded 200 keV. In this respect, also fusion neutron measurements could provide invaluable data for Z-pinch physics since they give insight into the acceleration of fast ions. Recently, the highest neutron yield from the $\mathrm{D}(d,\mathrm{n})^3\mathrm{He}$ fusion reaction of 6×10^{13} has been achieved with a double-shell deuterium gas puff on the 17 MA current level [4], [5]. With regard to the overall neutron yield in this experiment, there is a hope for a large thermonuclear component; however, an unambiguous evidence has not been yet provided.

The results previously mentioned indicate that there is a need of more experimental data about fast ions. For that purpose, we measured the production of fusion neutrons on the S-300 generator at the Kurchatov Institute in Moscow. We carried out Z-pinch experiments with: 1) deuterated fibers; 2) various types of wire arrays imploding onto a deuterated fiber; and 3) deuterium gas puffs as Z-pinch loads. Because results from fiber and wire-array Z-pinches have been already published in [6], in this paper, we particularly focus on experiments with deuterium gas puffs. The structure of this paper is the following: The experimental arrangement and diagnostics used in our experiment are described in Section II (the emphasis was put mainly on the comprehensive neutron time-of-flight (TOF) diagnostics). Section III provides the most important experimental results which are then discussed in Section IV. Finally, results are summarized in Section V.

II. Experimental Arrangement and Diagnostics

A. Experimental Setup

The implosion of a solid deuterium gas-puff Z-pinch was studied on the S-300 pulsed power generator (4-MA peak current, 700-kV voltage, 100-ns rise time, 0.15-Ω impedance) at the Kurchatov Institute in Moscow [7], [8]. This paper presents results from the experimental series of ten shots at the current level of 2 MA.

The gas-puff hardware was designed according to the gas valve used on the Angara-5 device [9]. A photograph of the gas-puff anode and cathode can be seen in Fig. 1. The separation between the cathode and the anode was 10 mm. The

Manuscript received July 25, 2008; revised October 3, 2008. First published February 10, 2009; current version published March 11, 2009. This work was supported in part by the Grant Agency of the Czech Republic under Grant 202-08-P084, by the Ministry of Education under Research Programs LA08024, ME09087, and LC528, and by the IAEA under Grant RC14817.

D. Klir, J. Kravarik, P. Kubes, and K. Rezac are with Czech Technical University in Prague, 166 27 Prague, Czech Republic (e-mail: klird1@fel.cvut.cz; kravarik@fel.cvut.cz; kubes@fel.cvut.cz; rezack@fel.cvut.cz).

S. S. Ananev, Y. L. Bakshaev, P. I. Blinov, A. S. Chernenko, E. D. Kazakov, V. D. Korolev, and G. I. Ustroev are with the Russian Research Center "Kurchatov Institute," 123182 Moscow, Russia (e-mail: seregin2000@mail.ru; bak@dap.kiae.ru; blinov@dap.kiae.ru; chernenko@dap.kiae.ru; evgenische@gmail.com; korolev@dap.kiae.ru; gustroev@dap.kiae.ru).

L. Juha and J. Krasa are with the Institute of Physics, Academy of Sciences of the Czech Republic, 182 21 Prague, Czech Republic (e-mail: juha@fzu.cz; krasa@fzu.cz).

A. Velyhan is with the Institute of Physics, Academy of Sciences of the Czech Republic, 182 21 Prague, Czech Republic (e-mail: velyhan@fzu.cz).

Color versions of one or more of the figures in this paper are available online at http://ieeexplore.ieee.org.

Digital Object Identifier 10.1109/TPS.2008.2010860

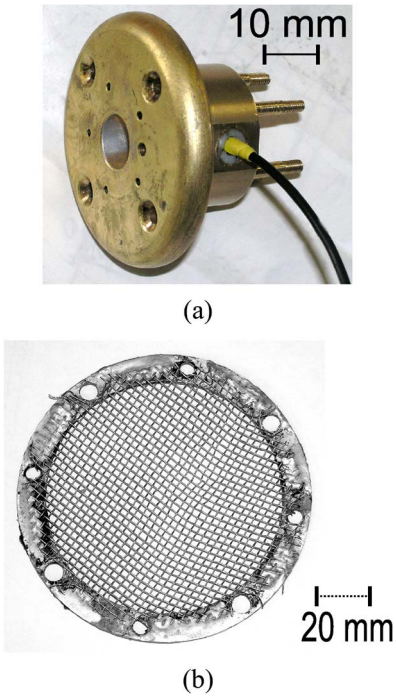

Fig. 1. Deuterium gas-puff hardware. (a) Cathode, gas-puff nozzle. (b) Anode, stainless steel mesh.

anode was formed by a stainless steel mesh. The gas puff was triggered by an electrical spark which ignited gunpowder. A Teflon piston driven by the burning gunpowder then compressed the deuterium gas in a closed volume below the nozzle. The deuterium gas entered the nozzle when the gas pressure broke through a 0.2-mm-thick stainless steel foil. The delay between the detection of the deuterium gas in the nozzle and the current generator start-up was set up between 10 and 40 μs. The outer diameter of the conical solid deuterium gas puff was 10 mm and about 15 mm at the cathode and at the anode, respectively. At the time of the current onset, we expected the line deuterium gas density of $5 \div 50$ μg/cm. The gas density profile has not been characterized so far since our primary intention was to implement and to test extended TOF method for the determination of neutron energy spectra [10], [11]. We would like to apply a high number of neutron TOF detectors in order to study the anisotropy of neutron energy distribution function in Z-pinch plasmas, and we used the deuterium gas puff as a suitable source of neutrons.

B. Diagnostics

In order to observe Z-pinch discharges that show specific experimental results in each shot, it is important to use simultaneously comprehensive diagnostics with temporal, spatial, and spectral resolution. The diagnostic setup, part of which was described in [12], is shown in Fig. 2.

First, in order to provide time and space resolved information about visible emission, a radial optical streak camera was used. The plasma 5 mm away from the cathode was imaged on the streak camera slit. Furthermore, an optical frame camera provided three 2-D images with 3-ns exposure and 20-ns interframe separation.

Second, X-ray radiation was detected with a pinhole camera and a semiconductor diode. The X-ray pinhole camera, time integrated and differentially filtered (with 2-μm Al, 10-μm Al, and 15-μm Cu filters), was used to observe the plasma in various spectral ranges with a spatial resolution of 100 μm. Time-resolved information about X-rays from 1 to 40 keV was obtained with the semiconductor diode SPPD11-4 [13].

Third, high-voltage and dI/dt probes provided information about electrical characteristics and the power input into a discharge. The load current was measured by current loops which were placed 6 cm from the Z-pinch axis.

Finally, neutron yields were measured with an indium activation counter and with thermoluminescent dosimeters which were placed inside 10-in-thick Bonner sphere, 1 m from the neutron source (cf., [14]). As far as the reconstruction of neutron energy spectra is concerned, it is the main subject of this paper, and therefore, neutron TOF analysis is presented separately in the following paragraphs.

C. Neutron TOF Diagnostics

Twelve fast plastic scintillators and photomultiplier tubes enabled the TOF analysis of fusion neutrons. All detectors were shielded by $1 \div 10$ cm of lead. The energy dependent sensitivity of neutron TOF detectors was calculated by the Monte Carlo N-Particle code [15]. The detector time resolution of about 4.5 and 5.0 ns was given mainly by the decay time of scintillators, by the electron transit time spread within the photomultiplier tube and by a neutron transit time through 5- and 10-cm-thick scintillators, respectively. Four axial (end-on) neutron detectors were located at distances of -5.07, -2.55 (the minus sign means upstream, i.e., at the top of the S-300 device, behind the anode), 2.55, and 7.43 m (downstream, i.e., at the bottom of the S-300 device, behind the cathode). We should make a note here that the term "downstream" does not mean the direction of current sheet acceleration as in plasma foci but the direction of current flow (from the anode toward the cathode). With regard to eight radial (side-on) detectors, they were positioned in two mutually perpendicular rows at distances of -8.31, -2.55, 2.55, and 8.31 m from the Z-pinch plasma (see Fig. 2). The choice of distances, where neutron TOF detectors were placed, fulfilled the following criteria.

First, it is necessary to place several neutron detectors as close to the neutron source as possible because the time of neutron production is estimated mainly from the nearest neutron signals. In our case, the time of neutron production was estimated from the nearest side-on TOF detectors at 2.55 m from the Z-pinch plasmas. The advantage of side-on detectors was smaller influence of scattered neutrons because side-on diagnostic ports of 10-cm diameter and 1.5-m length were surrounded by water (cf., scattered neutrons on the side-on and downstream detectors in Fig. 3). Another advantage of side-on detectors was the fact that neutron energy spectra were usually centered at about 2.45 MeV. Therefore, in order to obtain the temporal evolution of neutron emission, it was possible to shift the observed neutron signals at 2.55 m by the TOF of 2.45-MeV neutrons (which was about 118 ns, the temporal uncertainty was 2 ns). The temporal resolution (FWHM of pulse response) of

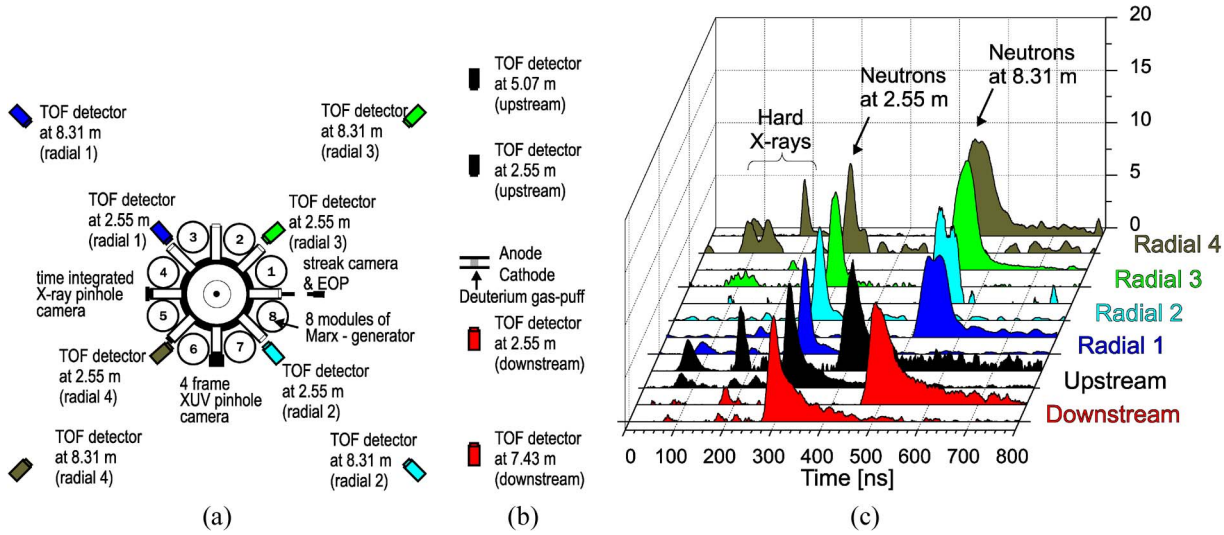

Fig. 2. Schematic diagram of our diagnostic setup with 12 TOF neutron detectors. (a) End-on view. (b) Side-on view. (c) Examples of neutron TOF signals in shot No. 070614-1, the neutron yield of about 2×10^9.

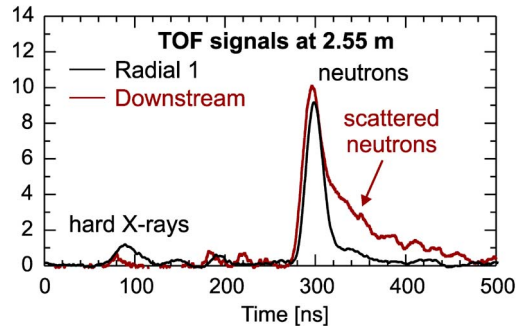

Fig. 3. TOF signals on the side-on (radial 1) and downstream detectors at 2.55 m, shot No. 070614-1, the neutron yield of about 2×10^9. Hard X-rays at about 100 ns were produced by current leakages before the gas-puff implosion.

neutron detection at 2.55 m was given mainly by the width of a neutron energy spectrum and was experimentally estimated below 10 ns.

Second, since energies of neutrons are determined mainly from the most distant detectors, several neutron TOF detectors were placed far from the experimental chamber. The neutron energy distribution function $f(E_{\rm n}, t)$ was reconstructed from time-resolved neutron signals $S(x, T)$ by the Monte Carlo method [6], [10], [16]. Including the temporal resolution of TOF detectors and neutron scattering, the systematic error of mean neutron energy estimated in our experiment was below 0.1 and 0.05 MeV for the end-on and side-on direction, respectively. As far as the error in the estimation of the width of neutron energy spectra is concerned, it was well below 100 keV (cf., downstream spectrum in Fig. 7). Of course, due to a low number of TOF detectors in a row, it was not possible to determine unambiguously the shape of neutron energy spectrum, nevertheless, the mean energy and the width of spectrum could be estimated.

Third, it is convenient to place detectors in various directions at the same distance. It enables instantaneous and unambiguous measurement of the neutron emission anisotropy (together with the anisotropy of the experimental arrangement) by simple comparison of TOF signals without any specific data processing such as the Monte Carlo simulation. The same distance is also useful for cross-calibration of detectors.

Fourth, neutron detectors can be used in mutually opposite directions (i.e., neutron spectra are evaluated from the chain of neutron detectors on the both sides of the neutron source). Such a procedure significantly improved results of neutron spectra reconstruction and limited the influence of scattered neutrons [6]. Besides that, it was possible to quantitatively estimate the role of scattered neutrons: The sum of the mean neutron energy in one direction and in the opposite direction should be about $2.45 + 2.45$ MeV $= 4.9$ MeV. If the sum is higher then 4.9 MeV, it can be caused by significant kinetic energies of fast deuterons. However, if the sum is lower, it is caused by lowering of neutron energies because of scattering.

The aforementioned set of diagnostic tools enabled us to observe results which are presented in the following section.

III. Experimental Results

A. Plasma Dynamics

We carried out a series of ten shots with a deuterium gas puff. The typical waveforms and images obtained are shown in Fig. 4. The times described in this paper refer to the start of a current when $t = 0$. All signals were adjusted to account for different transit times from each detector to oscilloscopes. The temporal uncertainty between waveforms of X-rays, neutrons, and electrical characteristics was below 5 ns.

The visible image in Fig. 4 recorded the conical shape of a deuterium gas puff. The conical implosion resulted also in the formation of a jet which was observed in the time-integrated X-ray pinhole image (see Fig. 5). The streak camera in Fig. 4 clearly showed the implosion of a deuterium gas puff. The implosion started at about 60 ns, and the velocity reached the modest value of 6×10^4 m/s. At about 150 ns, during the stagnation of deuterium plasmas on the axis, the voltage signal, hard X-ray emission, and neutron production peaked. The plasma

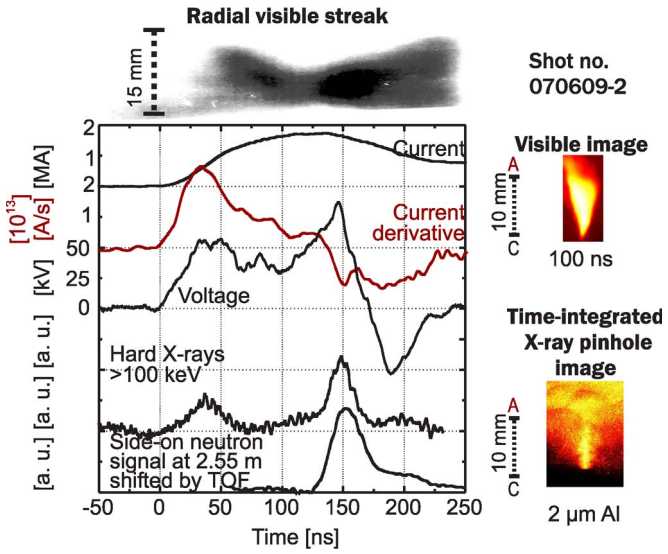

Fig. 4. Visible streak image, visible image, X-ray pinhole image and waveforms of current, current derivative, voltage, hard X-rays, and neutron emission recorded in discharge No. 070609-2, the neutron yield of about 4×10^9.

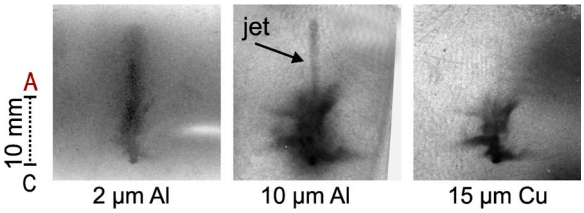

Fig. 5. Collimated jet above the anode in time integrated X-ray pinhole images in discharge No. 070614-1, the neutron yield of about 2×10^9.

impedance during the implosion and stagnation $R_P + \dot{L}_P = (V - L_P\dot{I})/I$ exceeded 0.04 Ω (in the shot with the highest neutron yield, the plasma impedance was about 0.15 Ω). A relatively low implosion velocity together with a small plasma impedance and inductance indicate that a significant part of the electric current was flowing near the return current post, i.e., near the radius of 5 cm. It is likely that this fact was caused by a large spread of the deuterium gas in the central anode–cathode region.

B. Time of Hard X-Ray and Neutron Production

X-ray emission started at the stagnation of a deuterium gas puff on the axis. In all shots, the peak of X-ray emission corresponded to a voltage spike and to a dip in a dI/dt signal. The hard X-ray emission lasted during the stagnation and expansion phase. As far as neutron peaks are concerned, they temporally correlated with hard X-ray peaks within 5-ns accuracy. The neutron pulse lasted on average 25 ± 10 ns (FWHM). The error of 10 ns represents the shot-to-shot variation and the variation between four nearest radial detectors.

C. Neutron Energy Distribution Function

Neutron energy spectra were reconstructed from TOF signals by the Monte Carlo simulation which was described in [6] and [16]. A typical example of neutron TOF signals detected with

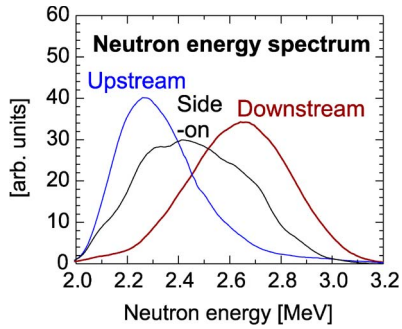

Fig. 6. End-on and side-on (radial 3) energy spectra of neutrons, shot No. 070614-1, the neutron yield of about 2×10^9.

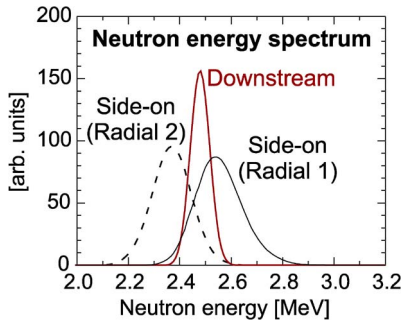

Fig. 7. End-on and side-on (radial 1 and 2) energy spectra of neutrons, shot No. 070605-1, the neutron yield of about 9×10^8.

12 detectors is shown in Fig. 2(c). In Fig. 6, we can see end-on and side-on neutron spectra obtained from these 12 waveforms. Each of the three spectra in Fig. 6 was reconstructed from 4 TOF detectors in a row.

On average, the side-on neutron energy peaked at 2.42 ± 0.04 MeV, and the FWHM of neutron energy spectra was 450 keV. In the downstream direction, the peak neutron energy and the width of a neutron spectrum were 2.60 ± 0.10 and 400 keV, respectively. In the upstream direction, the peak neutron energy was 2.30 ± 0.10 MeV.

As regards side-on neutron TOF signals at 8.31 m in Fig. 2 and the side-on neutron energy spectrum in Fig. 6, they showed a multipeak structure. It follows that time-integrated neutron energy spectra could be formed by a multiphase process. An interesting result was achieved in several other shots. For example, in shot No. 070605-1 (see Fig. 7), we observed a relatively narrow width of an end-on neutron energy spectrum together with an anisotropic emission in the side-on direction (see also radial 1 and radial 2 directions in Fig. 2). At this point, it should be noted that these results are not just artifacts of our Monte Carlo reconstruction. The radial anisotropy was evident even before any data were processed. Fig. 8 shows signals from radial TOF detectors at the same distance of about 8.31 m. Hard X-rays on the radial 1 detector coincided with the radial 2 detector (see Fig. 8). In most cases, also the temporal differences between neutron TOF signals were below the temporal uncertainty of about 3 ns. However, in this particular shot, the temporal difference was 13 ns. It means that most fusion reactions were really realized in the center of mass frame which was moving in the side-on direction (with respect to the laboratory frame of reference).

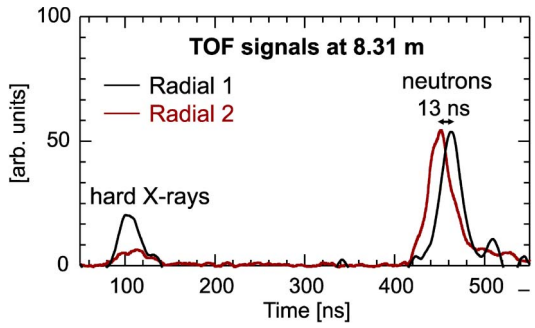

Fig. 8. TOF signals on the side-on detectors (radial 1 and 2) at 8.31 m, shot No. 070605-1, the neutron yield of about 9×10^8. Hard X-rays at about 100 ns were produced by current leakages before the gas-puff implosion.

D. Neutron Yield

We detected neutrons from D-D fusion reactions in eight cases over a series of ten shots. The peak neutron yield was achieved in the case of the highest plasma voltage of about 300 kV, the highest plasma impedance of 0.15 Ω, and the highest implosion velocity. The peak neutron yield exceeded 10^{10} on the current level of 2 MA.

On the one hand, such a number of neutrons was a common yield in fiber Z-pinch experiments [17]–[20]. The neutron yield of 10^{10} on 2-MA current level is also consistent with I^4 scaling and neutron yields obtained on the Saturn generator (2×10^{12} at 7.5 MA current [21]) and on the Z machine (3×10^{13} at 15 MA current [5]). However, on the other hand, neutron yields up to 10^{12} were achieved with a plasma focus [22] and with a gas-puff Z-pinch on the ANGARA-5-1 [9] on the current level of 2–3 MA. Therefore, it is possible that there are two different neutron production mechanisms, and we would like to focus on this issue during our future gas-puff experiments on the S-300 generator.

It would be interesting to know if we succeed in increasing the neutron yield with the gas-puff optimization on the S-300 generator. In our preliminary gas-puff experiments, we suppose that a significant current did not flow through the central part of a gas puff because of the large spread of a deuterium gas. In these cases, the plasma compression and subsequently the neutron yield were reduced. Even though the deuterium gas puff was not optimized for the highest neutron yield, these experiments confirmed our assumption that neutron yields with deuterium gas puffs are higher than with other Z-pinch configurations presented in [6] (on average, 5×10^8 for a deuterated fiber Z-pinch and 10^9 for a wire-array Z-pinch with an on-axis deuterated fiber).

IV. Discussion

A. Distribution Function of Deuteron Kinetic Energy Components

The knowledge of neutron spectra at different directions relative to the Z-pinch axis gives us important information about the energy of deuterons which produce fusion reactions. If energies of reacting deuterons are much smaller than the energy released from the $\mathrm{D}(d,\mathrm{n})^3\mathrm{He}$ fusion reaction (i.e., much lower than 3.3 MeV), the neutron energy is given mainly by the component of deuteron kinetic energy in the direction of neutron detection, and it is possible to transform neutron energy spectra into distribution functions of side-on and end-on energy components of deuterons (cf., [6]). Results obtained in shots previously mentioned are shown in Fig. 9.

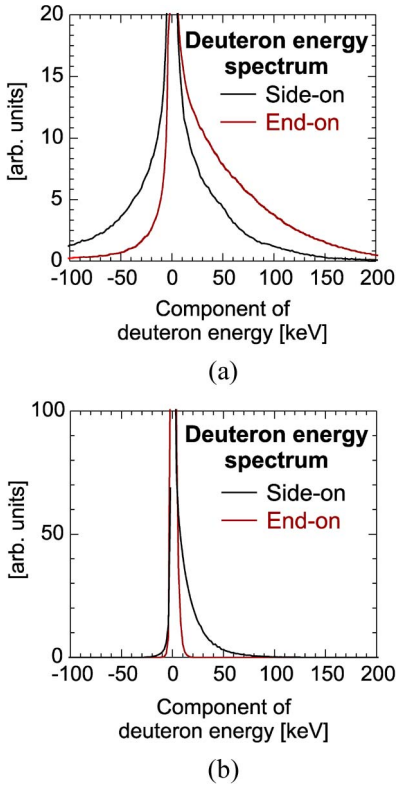

Fig. 9. Distribution functions of kinetic energy components of reacting deuterons. The plus and minus signs of kinetic energy component reflect the direction of deuteron velocity. (a) Shot no. 070614-1. (b) Shot no. 070605-1.

In Fig. 9(a), we can see that fusion neutrons were produced mainly by deuterons with a kinetic energy component below 100 keV. The mean axial component of the deuteron kinetic energy $\langle |E_\parallel| \rangle$ was 50 keV while the mean side-on component $\langle |E_\perp| \rangle$ was 35 keV. The average kinetic energy of reacting deuterons was $\langle E_\mathrm{d} \rangle = \langle E_x + E_y + E_z \rangle = 2\langle |E_\perp| \rangle + \langle |E_\parallel| \rangle \doteq 120$ keV. Our Monte Carlo reconstruction also estimated the downstream/upstream anisotropy of neutron flux as 1.1.

B. Generalized Beam-Target Model

If we are to discuss the neutron production mechanism in our gas-puff experiments, we should perhaps start with the discussion of an important result that was observed: the anisotropy of neutron energy spectra. The neutron emission anisotropy was most likely caused by a beam of fast deuterons which were accelerated in certain directions and thereafter collided with "cold" target deuterons. Usually, most of the fast deuterons were directed toward the cathode. We used such an orientation of the conical gas puff that a hydrodynamic flow occurred toward the anode, i.e., in the opposite direction than the one in which deuterons were directed. That is why it seems reasonable to explain the deuteron acceleration to 100 keV energies by the

diode action. However, in some shots, the anisotropy was also apparent in the side-on direction. This very fact leads us to a supposition that the deuteron acceleration and fusion neutron production is a rather complicated multiphase process which could result in broad widths of neutron energy spectra on the order of 400 keV. Such a broad width of neutron energy spectra then caused a relatively small anisotropy of neutron flux. Similar neutron energy spectra were obtained in our previous wire-array Z-pinch experiments on the S-300 generator (cf., [6]) as well as in plasma focus discharges [23], [24].

With regard to plasma focus discharges, a high radial component of deuteron velocities was explained by: 1) the Fermi acceleration mechanism and/or 2) the generalized beam-target model. In the Fermi acceleration mechanism, deuterons acquire the energy from the radially imploding current sheet [25] whereas in the generalized beam-target model (gyrating particle model), axially accelerated deuterons are bent by magnetic fields before they produce fusion neutrons [23], [26], [27].

With regard to our experiments, we can draw similar conclusions as in previous experiments on the S-300 generator (cf., [6]). The neutron emission anisotropy and the broad width of neutron spectra are the main arguments against the thermonuclear origin of neutrons. Furthermore, the observed radial neutron spectra could be explained neither by a monoenergetic deuteron beam nor by deuteron beams moving at a single angle to axis. The observed spectra have to be explained by a broad angular dependence and by monotonically decreasing energy dependence of deuteron energy distribution function. These conclusions are far from the simple concept of a linear beam-target model, and this is why Bernstein with his colleagues introduced the term generalized beam-target model [23]. On the basis of our experimental data, we are not able to decide how the beam of fast deuterons was created. Nevertheless, the aforementioned results put unambiguous restrictions on models of deuteron acceleration. For instance, the radial Fermi acceleration mechanism is inconsistent with spectra in Figs. 6 and 9(a) whereas it cannot be completely excluded in the shot with spectra in Figs. 7 and 9(b).

C. Plasma Voltage and Resistance

The discussion part of this paper shall be concluded by a description of the temporal correlation of neutron emission with plasma voltage, the characteristic feature of our experiment, and the issue of plasma resistance. The origin of voltage peaks during the neutron emission is discussed here because it could elucidate the process of accelerating fast deuterons. The positive voltage peaks could be explained by the plasma resistance R_{P}, by the increasing inductance $\dot{L}_{\mathrm{P}} > 0$ or by the increasing current $\dot{I} > 0$. In our experiment with a deuterium gas puff as well as in deuterium gas-puff experiments on the Angara 5-1 device at Troitsk [9], neutrons were emitted at the stagnation and at the beginning of plasma expansion. This means that the measured voltage peaks could be hardly ascribed to an increasing plasma inductance $\dot{L}_{\mathrm{P}}$. Furthermore, it is highly probable that the resistive voltage $R_{\mathrm{P}}I$ significantly contributed to voltage peaks because the induced voltage $L_{\mathrm{P}}\dot{I}$ was negative during the neutron emission.

On the Angara 5-1 generator, the plasma impedance was between 0.1 and 0.3 Ω. Such a value could not be explained by the Spitzer resistivity and the possibility of anomalous resistance was discussed. The characteristic feature of the experiment at Troitsk was the relatively small mass of a liner and the axial gradient of a linear density. Therefore, microturbulences were supposed to occur near the anode where the gas density was low.

The anomalous resistance does not seem to be a unique feature of a few experiments. The enhanced plasma resistance $(0.2 \div 0.4\ \Omega)$ during the neutron emission was measured also for a broad energy range of plasma focus machines [28], [29] and in our previous experiments on the S-300 generator [6]. As far as the gas-puff experiment described in this paper is concerned, the plasma impedance was usually below 0.05 Ω. However, the peak neutron yield was achieved in the case of plasma impedance of 0.15 Ω. Such a value does not indicate only that the resistance could play an important role in our gas-puff experiment but also that the enhanced resistance could be a general phenomenon in Z-pinches at the poststagnation phase.

V. Conclusion

The implosion of a deuterium gas-puff Z-pinch was studied on the S-300 generator. The emphasis was put mainly on the reconstruction of the neutron energy distribution function from 12 neutron TOF signals by the Monte Carlo simulation. The neutron measurements were used to obtain data about acceleration of deuterons in Z-pinch plasmas.

The peak neutron yield above 10^{10} was achieved on the current level of 2 MA. The fusion neutrons were generated at about 150 ns after the current onset and the emission lasted on average 25 ns. The side-on neutron energy spectra peaked at 2.42 ± 0.04 MeV with about 450-keV FWHM. In the downstream direction, the peak neutron energy and the width of a neutron spectrum were 2.6 ± 0.1 MeV and 400 keV, respectively. The average kinetic energy of fast deuterons, which produced fusion neutrons, was about 100 keV. The generalized beam-target model probably fits best to the obtained experimental data.

In future experimental campaigns, we shall pay special attention to the reduction of a deuterium gas spread in the energy concentrator and to the optimization of a deuterium gas puff. We would like to increase the neutron yield and to measure the gas-puff density profile. This, we believe, is necessary for further experimental data processing and for the subsequent discussion of deuteron acceleration mechanisms.

Acknowledgment

The authors would like to thank Prof. A. S. Kingsep for his valuable comments and Dr. G. N. Timoshenko (Laboratory of Radiation Biology of JINR, Dubna) for his kind assistance with Bonner spheres. The authors would also like to thank M. Kralik (Czech Metrology Institute) for his help with the MCNP code.

REFERENCES

[1] T. Sandford, G. Allshouse, B. Marder *et al.* "Improved symmetry greatly increases X-ray power from wire-array Z-pinches," *Phys. Rev. Lett.*, vol. 77, no. 25, pp. 5063–5066, Dec. 1996.

[2] R. Spielman, C. Deeney, G. Chandler *et al.*, "Tungsten wire-array Z-pinch experiments at 200 TW and 2 MJ," *Phys. Plasmas*, vol. 5, no. 5, pp. 2105–2111, May 1998.

[3] M. G. Haines, P. D. LePell, C. A. Coverdale, B. Jones, C. Deeney, and J. P. Apruzese, "Ion viscous heating in a magnetohydrodynamically unstable Z-pinch at over 2×10^9 kelvin," *Phys. Rev. Lett.*, vol. 96, no. 7, p. 075 003, Feb. 2006.

[4] A. L. Velikovich, R. W. Clark, J. Davis *et al.*, "Z-pinch plasma neutron sources." *Phys. Plasmas*, vol. 14, no. 2, pp. 022 701-1–022 701-16, Feb. 2007.

[5] C. A. Coverdale, C. Deeney, A. L. Velikhovich *et al.*, "Neutron production and implosion characteristics of a deuterium gas-puff Z pinch," *Phys. Plasmas*, vol. 14, no. 2, pp. 022 706-1–022 706-7, Feb. 2007.

[6] D. Klir, J. Kravarik, P. Kubes *et al.*, "Neutron emission generated during wire array Z-pinch implosion onto deuterated fiber," *Phys. Plasmas*, vol. 15, no. 3, pp. 032 701.1–032 701.13, Mar. 2008.

[7] A. S. Chernenko, Y. M. Gorbulin, Y. G. Kalinin *et al.*, "S-300, new pulsed power installation in Kurchatov Institute, investigation of stable liner implosion," in *Proc. 11th Int. Conf. High Power Particle Beams*, J. Ullschmied, Ed. Prague, Czech Republic: Acad. Sci. Czech Republic, 1996, vol. 1, p. 154.

[8] Y. L. Bakshaev, A. S. Chernenko, V. D. Korolev *et al.*, "Energy concentration on S-300 pulsed power generator," in *Proc. 11th Int. Conf. High Power Particle Beams*, J. Ullschmied, Ed. Prague, Czech Republic: Acad. Sci. Czech Republic, 1996, vol. 2, p. 962.

[9] A. V. Batyunin, A. N. Bulatov, V. D. Vikharev *et al.*, "Study of an ultrafast Z-pinch on the Angara 5-1 device," *Sov. J. Plasma Phys.*, vol. 16, pp. 597–601, 1990.

[10] I. Tiseanu, G. Decker, and W. Kies, "A Monte-Carlo technique for the reconstruction of time dependent spectra of short-pulse neutron sources," *Nucl. Instrum. Methods Phys. Res. A, Accel. Spectrom. Detect. Assoc. Equip.*, vol. 373, no. 1, pp. 73–80, Feb. 1996.

[11] I. Tiseanu and I. Craciunescu, "Evaluation of reconstruction methods for time-resolved spectroscopy of short-pulsed neutron sources," *Nucl. Sci. Eng.*, vol. 122, no. 3, pp. 384–394, 1996.

[12] Y. L. Bakshaev, P. I. Blinov, A. S. Chernenko *et al.*, "Diagnostic arrangement on S-300 facility," *Rev. Sci. Instrum.*, vol. 72, no. 1, pp. 1210–1213, Jan. 2001.

[13] Y. L. Bakshaev, P. I. Blinov, V. V. Vikhrev *et al.*, "Measurements of neutron emission from a Z-pinch constriction," *Plasma Phys. Rep.*, vol. 32, no. 7, pp. 531–538, Jul. 2006.

[14] A. Velyhan, J. Krasa, B. Bienkowska *et al.*, "Use of thermoluminescent dosimeters for measurement of fast-neutron spatial-distribution at the plasma focus device PF-1000," *Phys. Scr.*, vol. T123, pp. 66–78, Mar. 2006.

[15] J. F. Briesmeister, "MCNP—A general Monte Carlo N-particle transport code," Los Alamos Nat. Lab., Los Alamos, NM, Report No. LA-12625-M, 1993.

[16] K. Rezac, D. Klir, P. Kubes, J. Kravarik, and M. Stransky, "Monte Carlo simulations for reconstruction of neutron time-resolving energy distribution in D-D fusion reactions," *Czech J. Phys.*, vol. 56, pp. B357–B363, Oct. 2006.

[17] F. Young, S. Stephanakis, and D. Mosher, "Neutron and energetic ion production in exploded polyethylene fibers," *J. Appl. Phys.*, vol. 48, no. 9, pp. 3642–3650, Sep. 1977.

[18] J. D. Sethian, A. E. Robson, K. A. Gerber, and A. W. DeSilva, "Enhanced stability and neutron production in a dense Z-pinch plasma formed from a frozen deuterium fiber," *Phys. Rev. Lett.*, vol. 59, no. 8, pp. 892–899, Aug. 1987.

[19] W. Kies, G. Decker, M. Malzig *et al.*, "Terawatt fiber pinch experiments," *J. Appl. Phys.*, vol. 70, no. 12, pp. 7261–7272, Dec. 1991.

[20] V. V. Vikhrev and V. D. Korolev, "Neutron generation from Z-pinches," *Plasma Phys. Rep.*, vol. 33, no. 5, pp. 356–380, May 2007.

[21] R. Spielman, G. Baldwin, G. Cooper *et al.*, "D-D fusion experiments using fast Z-pinches," Sandia Nat. Lab., Albuquerque, NM, Rep. SAND98-07-05, 1998.

[22] A. Bernard, J. P. Garconnet, A. Jolas, J. P. Le Breton, and J. de Mascureau, "Turbulence caused by the interaction between plasma and electric current in the focus experiment," in *Proc. 7th IAEA Conf. Plasma Phys. Controlled Nucl. Fusion, Innsbruck, 1978—Plasma Physics and Controlled Fusion Research (IAEA-CN-37)*. Vienna, Austria: IAEA, 1979, vol. 2, pp. 159–172.

[23] M. J. Bernstein and G. G. Comisar, "Neutron energy and flux distributions from a crossed-field acceleration model of plasma focus and Z-pinch discharges," *Phys. Fluids*, vol. 15, no. 4, pp. 700–707, Apr. 1972.

[24] A. Bernard, A. Coudeville, A. Jolas, J. Lauspach, and J. de Mascreau, "Experimental studies of the plasma focus and evidence for nonthermal processes," *Phys. Fluids*, vol. 18, no. 2, pp. 180–194, Feb. 1975.

[25] R. Deutsch and W. Kies, "Ion acceleration and runaway in dynamical pinches," *Plasma Phys. Control. Fusion*, vol. 30, no. 3, pp. 263–276, Mar. 1988.

[26] U. Jager and H. Herold, "Fast ion kinetics and fusion reaction-mechanism in the plasma-focus," *Nucl. Fusion*, vol. 27, no. 3, pp. 407–423, 1987.

[27] V. A. Gribkov, A. Banaszak, and B. Bienkowska *et al.*, "Plasma dynamics in the PF-1000 device under full-scale energy storage: II. Fast electron and ion characteristics versus neutron emission parameters and gun optimization perspectives," *J. Phys. D, Appl. Phys.*, vol. 40, no. 12, pp. 3592–3607, Jun. 2007.

[28] G. Decker, W. Kies, and G. Pross, "The first and the final fifty nanoseconds of a fast focus discharge," *Phys. Fluids*, vol. 26, no. 2, pp. 571–578, Feb. 1983.

[29] A. Bernard, "Recent developments in plasma focus research," *Atomkernenergie*, vol. 32, pp. 73–75, 1978.

Daniel Klir was born in Podebrady, Czech Republic, on March 4, 1979. He received the M.Sc. degree in applied physics and the Ph.D. degree in plasma physics from Czech Technical University in Prague (CTU), Prague, Czech Republic, in 2002 and 2005, respectively.

Since 2005, he has been a Research Associate with the Department of Physics, Faculty of Electrical Engineering, CTU. His research interests include Z-pinch physics and plasma diagnostics based on X-ray and neutron detection.

Jozef Kravarik was born in Bosaca, Slovakia, on August 9, 1936. He received the M.Sc. degree in electrical engineering and the Ph.D. degree in plasma physics from Czech Technical University in Prague (CTU), Prague, Czech Republic, in 1960 and 1967, respectively.

Since 1963, he has been with the Faculty of Electrical Engineering, CTU, where he has been an Associate Professor since 1976. His research activities concentrate on the visual, X-ray, laser, and high-energy particle diagnostics of the Z-pinch and plasma focus discharges.

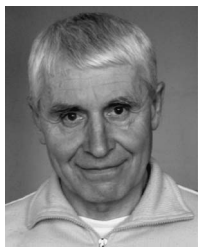

Pavel Kubes (M'07) was born in Prague, Czech Republic, on May 23, 1943. He received the M.Sc. degree from the Charles University, Prague, and the Ph.D. degree in plasma physics from Czech Technical University in Prague (CTU), Prague, in 1965 and 1977, respectively.

Since 1966, he has been with the Department of Physics, Faculty of Electrical Engineering, CTU, where he has been a Professor of applied physics since 1991. His research interests concentrate on the study of X-rays and neutrons in Z-pinch and plasma focus discharges.

Karel Rezac was born in Kladno, Czech Republic, on June 16, 1980. He received the M.Sc. degree in computer science and engineering from Czech Technical University in Prague, Prague, Czech Republic, in 2004, where he is currently working toward the Ph.D. degree in the Faculty of Electrical Engineering.

His research interests include plasma diagnostics and numerical simulations in neutron diagnostics.

Sergey S. Ananev was born in Moscow, Russia, in 1982. He received the M.Sc. degree in physics from Moscow Institute of Natural Sciences and Ecology, Moscow, in 2005.

Since 2002, he has been with the Russian Research Center "Kurchatov Institute," Moscow, working in the field of X-ray and EUV plasma spectroscopy and plasma visualization with the time resolution. His research interests include Z-pinch and plasma diagnostics based on laser probing and electooptical systems.

Yuriy L. Bakshaev was born in Jaransk, Russia, on July 31, 1938. He received the degree in radio physics and electronics from NNGU in Gorki in 1960.

Up to 1969, was with VNIIF in Snezhinsk as the Senior Engineer. Since 1969, he has been with the Russian Research Center "Kurchatov Institute," Moscow, Russia, as a Senior Scientist. His scientific interests include the physics of hot dense Z-pinch plasma and engineering of powerful pulse accelerators.

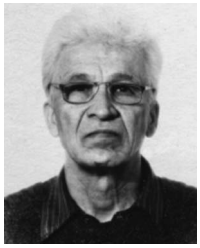

Peter I. Blinov was born in Russia in 1932. He received the M.Sc. degree in technical physics from Leningrad Polytechnic Institute, Saint Petersburg, Russia, in 1955.

Since 1976, he has been with the Russian Research Center "Kurchatov Institute," Moscow. In 1971, he became an Associate Professor with Kharkov University, Kharkov, Russia. His research interests include Z-pinch and plasma diagnostics.

Andrey S. Chernenko was born in Moscow, Russia, in 1951. He received the degree in physics from Moscow Institute of Physics and Technologies, Moscow, in 1974 and the Ph.D. degree from the Kurchatov Institute of Atomic Energy, Moscow, in 1984.

Since 1974, he has been with the Russian Research Center "Kurchatov Institute," Moscow, working in the field of intense electron beams and plasma diagnostics. His research interests include high-power current generators, Z-pinch, and plasma diagnostics.

Evgeny D. Kazakov was born in Moscow, Russia, in 1982. He received the degree in physics from Moscow Engineering Physics Institute (State University), Moscow, in 2005 and the Ph.D. degree from the Alikhanov Institute for Theoretical and Experimental Physics, Moscow, in 2008.

Since 2003, he has been with the Russian Research Center "Kurchatov Institute," Moscow, working in the field of X-ray and EUV plasma spectroscopy and plasma visualization. His research interests include Z-pinch and laser plasma physics and diagnostics.

Valery D. Korolev was born in Moscow, Russia, in 1943. He received the degree in physics from Moscow Engineering Physics Institute (State University), Moscow, in 1967 and the Ph.D. and Doctor of Science degrees from the Russian Research Center "Kurchatov Institute," Moscow, in 1978 and 2004, respectively.

His research interests include physics of relativistic electron beams, Z-pinch physics, and diagnostics of dense plasma.

Gennadiy I. Ustroev was born in Volsk, Russia, in 1941. He received the degree in physics from Moscow Engineering Physics Institute (State University), Moscow, Russia, in 1972.

Since 1970, he has been with the Russian Research Center "Kurchatov Institute," Moscow. His research interests include neutron physics, physics of fission, and structure of nuclei. Recently, his interests have included also Z-pinch physics, and the study of X-rays and neutrons produced by Z-pinches.

Libor Juha was born in Krnov, Czech Republic, on February 28, 1964. He received the M.Sc. and Ph.D. degrees from Czech Technical University in Prague, Prague, Czech Republic, in 1987 and 1995, respectively.

Since 1992, he has been a staff member with the Laser Plasma Department, Institute of Physics, Academy of Sciences of the Czech Republic, Prague. His research interests include interaction of intense XUV/X-ray radiation with matter, radiometry of intense short-wavelength radiation, and laser-plasma chemistry.

Josef Krasa was born in Borotice, Czech Republic, in 1946. He received the M.Sc. degree in experimental physics from the Charles University, Prague, Czech Republic, in 1969 and the Ph.D. degree in plasma physics from the Czechoslovak Academy of Sciences, 1977.

Since 1970, he has been with the Institute of Physics, Academy of Sciences of the Czech Republic, Prague. As a Senior Scientist, he was involved in the diagnostics of ions emitted from laser-produced plasmas, mainly in the analysis of time-of-flight spectra of pulsed ion currents. Moreover, he is interested in the neutron diagnostics with the use of thermoluminescent dosimeters in the PF-1000 Facility, IPPLM, Warsaw.

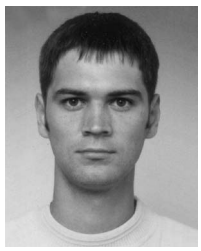

Andriy Velyhan was born in Uzhgorod, Ukraine, in 1976. He received the M.Sc. degree in physics from Uzhgorod State University, Uzhgorod, Ukraine, in 1999 and the Ph.D. degree from the Charles University, Prague, Czech Republic, in 2008. The topic of his doctoral thesis relates to the secondary emission and field emission from micrometer-size cosmic grains.

He is currently with the Institute of Physics, Academy of Sciences of the Czech Republic, Prague, where he is involved in the research of laser-induced highly charged ion beams and detection of neutron radiation by means of thermoluminescent dosimetry.